

Assessment of Trap Parameters Related with Thermoluminescence Peaks in BGO Single Crystals Doped with Vanadium

N. Uzunov, H. Hristov, V. Velev, N. Arhangelova, V. Bozadzhiev, D. Nedeva, I. Penev

Abstract — Doped $\text{Bi}_4\text{Ge}_3\text{O}_{12}$ (BGO) crystals possessing optical properties such as stimulated luminescence are largely exploited at present for many practical applications. We have conducted detailed studies on the thermally stimulated luminescence of some doped single crystals of BGO. Vanadium-doped (BGO:V) and ruthenium-doped (BGO:Ru) crystals have been grown in the Institute of Solid State Physics at the Bulgarian Academy of Sciences. The crystals have been irradiated with UV light from XBO lamp. Glow curves from BGO:V and BGO:Ru have been acquired using a precise thermoluminescence reader designed in the Laboratory for Nuclear physics and radioecology at the University of Shumen. A computerized glow curve deconvolution method has been exploited to obtain trap parameters of the two crystals. Fading of the peaks for the two types of crystals has been studied for time periods as large as 20 days. No significant time-dependence in peak positions and other trap parameters have been observed so far. Applications of the crystals for beta- and gamma- dosimetric applications have been reviewed.

Keywords: Thermoluminescence, trap parameters, glow curve deconvolution, activation energy, doped BGO, in-situ-, in-vivo dose measurements.

I. INTRODUCTION

Luminescence of crystals doped with different elements is very interesting in view of possible practical applications. The effect of thermoluminescence in particular is largely exploited at present in many applications in dosimetry, in nuclear medicine, in environmental studies, etc. There is a considerable amount of commercially available thermoluminescence phosphors with a large area of applications at present [1-4]. The doped crystals of $\text{Bi}_4\text{Ge}_3\text{O}_{12}$ (BGO) however, are of particular interest because they possess some very suitable properties. Bismuth Germanate

crystals, known also as Eluting, have physical and mechanical properties very suitable for dissymmetric purposes: they are colorless, transparent (from 300 to 6000 nm) and possess high mechanical, chemical, thermal and radiation stability. An important property for the applications is that they are insoluble in water and hence are suitable for dosimetric measurements in media with presence of dust and other impurities. The energy gap of pure BGO crystal has a relatively large value of 4.14 eV which determines a matrix very suitable for extrinsic elements [Pet]. An appropriate choice of the dopant such as for example transition metals or rare-earth elements could improve their sensitivity with respect to the beta- gamma- or ultraviolet radiation [Nik].

Some studies about the influence of vanadium on the optical properties and the magneto-optical effect in BGO crystals after preliminary thermal annealing or illumination treatments has already been conducted [Pet]. We have stressed our attention on the thermoluminescence studies of the properties of vanadium-doped $\text{Bi}_4\text{Ge}_3\text{O}_{12}$ (BGO:V) and ruthenium-doped $\text{Bi}_4\text{Ge}_3\text{O}_{12}$ (BGO:Ru) as potential candidates for long-term measurements of the ultraviolet region of solar emission as well as for in situ and in vivo dosimetric studies [6]. In this article we present the results from the computerized analysis of the thermoluminescence glow curves obtained under different irradiation conditions.

II. EXPERIMENTAL

Single crystals of BGO:V and BGO:Ru have been synthesized in the Institute of Solid State Physics, Bulgarian Academy of Sciences, with an automatic diameter-weight control system using the Czochralski technique.

Two thermoluminescence measuring setups have been used to obtain the physical parameters of the crystal: a setup for precise TL measurements developed in the Laboratory for nuclear physics and radioecology (LNPR) at the University of Shumen [3] and a standard TL reader Universal TOLEDO 654 (Vinten Instruments Ltd., UK) of the Laboratory for Radiopharmaceuticals and Biomolecular Imaging (LRBI) at the National Laboratories of Legnaro, INFN.

The first setup has been used to measure the crystal TL glow-curve obtained after irradiation with UV light. A block diagram of the setup is shown in Fig. 1. A photomultiplier tube (PMT) EMI type 9524A measures the light emitted from the crystal (CR) when the mechanical obturator (MO) is open. An electric resistance heater (ERH) is used to heat the crystal. It allows heating of crystals with dimensions up to $10 \times 10 \times 1 \text{ mm}^3$ and is operated by a heat control unit (HCU). The linear temperature increase is achieved using an appropriate regulation of the current of the heater from the voltage power supply (PS).

Revised Manuscript Received on 30 March 2015.

* Correspondence Author

Prof. N. Uzunov*, Laboratori Nazionali di Legnaro, Istituto Nazionale di Fisica Nucleare, Viale dell'Università 2, 35020 Legnaro (PD), Italy

Ass. Prof. Hristo Y. Hristov, Faculty of Natural Sciences, Konstantin Preslavsky University, Shumen, Bulgaria.

Ass. Prof. Valentin L. Velev, Faculty of Natural Sciences, Konstantin Preslavsky University, Shumen, Bulgaria.

Ass. Prof. Nina Arhangelova, Faculty of Natural Sciences, Konstantin Preslavsky University, Shumen, Bulgaria.

Assist. Prof. Ventsislav Bozadzhiev, Faculty of Natural Sciences, Konstantin Preslavsky University, Shumen, Bulgaria.

Assist. Prof. D. Nedeva, Technical University of Gabrovo, Gabrovo, Bulgaria.

Ass. Prof. I. Penev, Institute for Nuclear Research and Nuclear Energy, Shiptchenski prohod 69, 1574 Sofia, Bulgaria.

© The Authors. Published by Blue Eyes Intelligence Engineering and Sciences Publication (BEIESP). This is an open access article under the CC-BY-NC-ND license <http://creativecommons.org/licenses/by-nc-nd/4.0/>.

The thermometer TM1 registers the crystal temperature and the thermo sensor TM2 measures the temperature of the surrounding air.

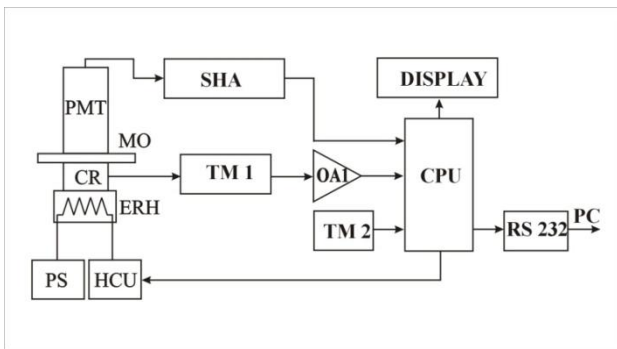


Fig.1 Block-diagram of the experimental setup

The central processor unit (CPU) fully controls the operations of the instrument. Its functions are realized by a PIC microcontroller type 16F876 [5]. The PIC registers the PMT pulses after being amplified and shaped to TTL voltage levels in the shaping amplifier SHA. The CPU controls the heating as well. It collects and converts into digital the signal from the thermometer TM1 which is amplified using an operational amplifier OA1 and also receives digital signal from the TM2. The information from the PIC can be transferred to a PC by a standard serial interface RS232C.

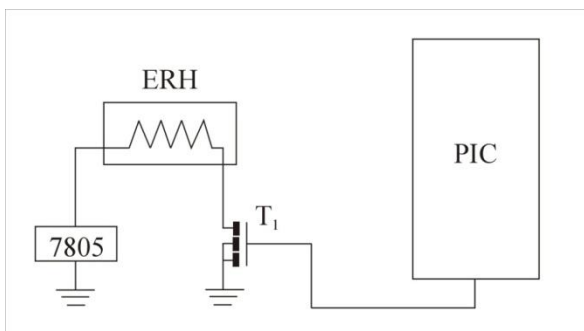


Fig. 2 Block diagram of the crystal heater current control

The current through the heater is controlled by the PIC digitally, using pulse width modulation (PWM) method (Fig. 2). The gate of the transistor T_1 (type BUZ11 [6]) receives from the PIC periodical pulse series with a frequency of 1 kHz. During each pulse T_1 is opened and the current flows from the stabilized voltage power supply unit 7805 through the heater and through T_1 to earth. The width of the pulses can be regulated by the PIC in the interval from zero to the maximum value in 256 steps, thus fixing 256 different values of the heating current.

The operational temperature range is chosen relatively large – from 30 to 300 °C in order to be able to conduct different crystal type's studies and the rate of its linear increase is 10 degree per minute [5]. Starting with from some initial value the pulse-width from PWM is changed at the end of each minute (60 seconds) so that a linear increase of the temperature in that time interval is achieved.

An original method of successive approximation is used to determine the PWM pulse-width values to perform the linear increase of the temperature. At the beginning a series of 28 linearly increasing PWM pulse-width values are set, so that a temperature increase from 30 °C to 300 °C is reached

for certain time interval. Then the functional dependence between used PWM values and the temperature measured corresponding to each PWM value is determined using a standard approximation procedure. From this function new series of PWM values are calculated subsequently, corresponding to the exact values of the temperature (40, 50, ..., 300 °C) at the end of each minute. Furthermore the same procedure of measurements, approximations and new PWM calculations are repeated until a satisfying linear dependence between the temperature and the time is achieved. After each iteration step this linearity is also evaluated. Normally the necessary precision is achieved in 4 iterations.

It has been obtained experimentally that the best approximation function is the exponential one:

$$PWM = a + b \exp\left(-\frac{T}{c}\right)$$

where: T is the temperature (in degree Celsius); parameters a, b, c are the fitting parameters ensuring a maximum of the correlation factor and minimum of the fit's standard deviation after each iteration step.

Following the procedure described above an experiment on the determination of the temperature linearity versus the heating time intervals has been conducted. The temperatures measured at calculated PWM values after the 4th iteration (at 14 °C ambient air temperatures) are shown in Table 1.

A very important problem is the stabilization of the linear temperature-to-time dependence with respect to the variations of the environmental parameters. As a result of a number of test experiments we have found, that the only parameter influencing significantly the heating process is the ambient temperature. The analysis shows that these fluctuations are less than 0.4 %, which is around the limit of the thermometer precision (0.5 %) and hence can be neglected.

These results show that the ambient temperature conditions introduce in the heater temperature variations as big as 2 °C and hence it is necessary to impose corresponding corrections in the PWM values. A simple way to solve the problem was to prepare 8 different table data with PWM values (using the successive approximation method described above) – one for each value of the ambient temperature shown in Table 3. These table data were memorized in the PIC which chooses the appropriate set according the reading from TM2.

A xenon short-arc lamp type XBO 75 W/2 from OSRAM has been used to irradiate the crystals with UV rays.

The second setup has been modified in order to extract the measured glow-curve yield data versus the temperature and was used to obtain the crystal TL curves after irradiation with liquid gamma-ray emitting ^{99m}Tc and gamma-ray and beta-ray emitting ¹⁸⁸Re. Analysis of the obtained glow curves has been carried out using a multi-component glow-curve deconvolution program, developed at LNPR [4].

III. GLOW CURVE DECONVOLUTION ANALYSIS

The intensity of a single glow peak of a general order of kinetics is described by the equation [6]:

$$I(T) = I_m b^{\frac{b}{b-1}} \exp\left[\frac{E}{kT} \cdot \frac{T-T_m}{T_m}\right] \times \left[(b-1)(1-\Delta) \frac{T^2}{T_m^2} \exp\left[\frac{E}{kT} \cdot \frac{T-T_m}{T_m}\right] + Z_m \right]^{\frac{b}{b-1}} \quad (1)$$

where $I(T)$ is the glow-peak intensity, I_m is the maximum glow-curve intensity, E (in electron-volts, eV) is the activation energy, k is the Boltzmann constant, T is the temperature (in Kelvin, K), T_m (in K) is the value of the temperature at the peak maximum, with $\Delta = 2kT/E$, $\Delta_m = 2kT_m/E$ and $Z_m = 1 + (b-1)/\Delta_m$. In (1) the parameter b is the so-called kinetic order. Equation (1) transforms to the well-known equations describing the first kinetic order or second kinetic order depending whether b is equal to 1 or 2 respectively [1]. In practice however, there are also intermediate states, described by the non integer values of b between 1 and 2.

Kinetic parameters such as the activation energy and the kinetic order are obtained using computerized glow curve deconvolution (GCD) analysis. When the glow peak is a composite peak, compounded by m overlapping glow peaks, the method consists of a minimization of the χ^2 -function

$$\chi^2 = \sum_{i=1}^n \left(I_i - \sum_{j=1}^m I_j(T_j) \right)^2 \quad (2)$$

where I_i are the measured glow-curve intensity values, $I_j(T_j)$ are the values of each partial glow curve at the temperature T_j , n is the number of the experimental points and m is the number of the partial glow peaks compounding the observed peak.

IV. MEASUREMENTS AND ANALYSIS OF THE EXPERIMENTAL DATA

The BGO:V crystal was sealed in a small nylon container and was placed for 48 hours in a vial filled with 20 ml of solution of ^{99m}Tc ($E_\gamma=141\text{keV}$, $T_{1/2}=6.1\text{h}$) with initial activity of 20mCi. A glow curve of the crystal thus irradiated with a dose of 0.56Gy is shown in Fig. 1 (thick black line). The heating rate during the GC acquisition was 0.5deg/s. The overlapping white line in the figure represents the GC fit (figure-of-merit = 0.7%) composed by four main peaks, indicated with numbers from 1 to 4 in the same figure.

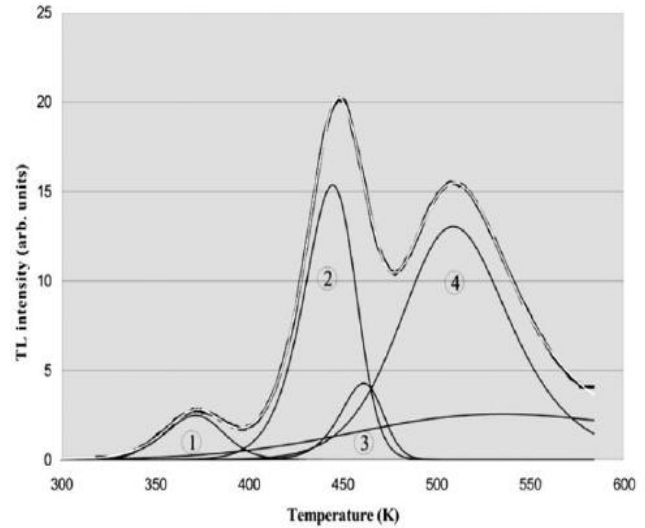


Fig.3: Glow curve shape of BGO:V obtained immediately after irradiation with gamma-ray emitting ^{99m}Tc

The crystal was irradiated for 17 hours in the same geometry using 20ml solution containing ^{188}Re ($E_\gamma=155\text{keV}$ and $E_{\beta_{\text{max}}}=2.12\text{MeV}$, $T_{1/2}=16.9\text{h}$). A glow curve of the crystal thus irradiated with a total dose of 1.1Gy is shown in Fig. 2 (thick black line). The heating rate during the data acquisition was 0.5deg/s. The overlapping white line represents the GC fit composed by four peaks from 1 to 4 in the figure. The comparison between the two GC shows a well-pronounced difference for the peak-area ratios between peak 2 and peak 4 in both cases.

A glow-curve deconvolution analysis of the BGO:V crystal irradiated with UV light and kept at different times at a constant temperature of 20 °C in a dark storage, has been

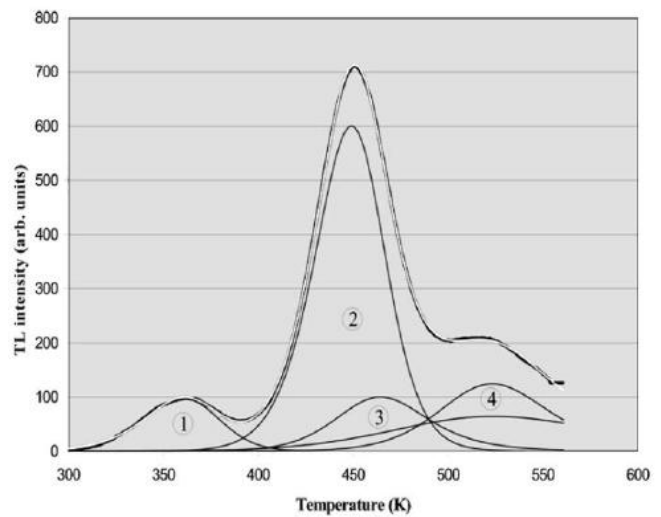


Fig.4: Glow curve shape of BGO:V obtained immediately after irradiation with gamma-ray and beta-ray emitting ^{188}Re

conducted. The resulting composite GC revealed a similar peak shape. For the observed maximum storage time a time-dependence of the peak area (fading) has been observed only for peak 1. Calculated crystal kinetic parameters from the measured values are shown in Table1.

TABLE 1: Obtained kinetic parameters for BGO: V

Peak reference	T _m (K)	Activation energy E (eV)	Kinetic order b
1	372 ± 2.3	0.94 ± 0.04	1.2 ± 0.1
2	450 ± 2.0	1.36 ± 0.08	1.7 ± 0.11
3	470 ± 6.1	1.70 ± 0.64	1.3 ± 0.38
4	492 ± 3.9	0.52 ± 0.09	1.4 ± 0.3

IV. DISCUSSION AND CONCLUSION

Analysis of the results obtained for the parameters of BGO:V shows that the crystal possess an acceptable sensitivity and could be exploited for *in-vivo* measurements of the absorbed dose of small animals treated with ¹⁸⁸Re and ^{99m}Tc. The difference between the peak area ratios between peak 2 and 4 is most probably due to the emission of beta-rays from ¹⁸⁸Re. This fact could be used to assess the partial dose caused by the beta rays when ¹⁸⁸Re is used.

ACKNOWLEDGEMENTS

Part of the present work has been supported by Grant-2015 from Fund for Scientific Research of Konstantin Preslavsky University, Shumen.

REFERENCES

1. J. L. Humm, A. Rosenfeld, A. Del Guerra, From PET detectors to PET scanners, *Eur. J. Nucl. Med. Mol. Imaging*, Vol 30, No 11 (2003), pp 1574 – 1597 Available: <http://link.springer.com/article/10.1007/s00259-003-1266-2>
2. N. K. Doshi, R. W. Silverman, Y. Shao, S. H. Cherry, maxPET: a dedicated mammary and axillary region PET imaging system for breast cancer, *IEEE Trans. Nucl. Sci.*, Vol 48, (2001), pp 811 – 815 Available: http://ieeexplore.ieee.org/xpl/articleDetails.jsp?arnumber=940168&sortType%3Dasc_p_Sequence%26filter%3DAND%28p_IS_Number%3A20355%29
3. W. Enghardt, P. Crespo, F. Fiedler, R. Hinz, K. Parodi, J. Pawelke, F. Ponish, 2004 Charged hadron tumour therapy monitoring by means of PET, *Nucl. Instr. Meth. Phys. Res., A* 525 (2004), pp 284 – 288 Available: <http://www.sciencedirect.com/science/article/pii/S0168900204004218>
4. M. Tsuchimochi, H. Sakahara, K. Hayama, M. Funaki, R. Ohno, T. Shirahata, T. Orskaug, G. Maehlum, K. Yoshioka, E., Nyard, A prototype small CdTe gamma camera for radioguided surgery and other imaging applications, *Eur. J. Nucl. Med. Mol. Imaging*, Vol 30, No 12 (2003), pp 1605 – 1614 Available: <http://link.springer.com/article/10.1007/s00259-003-1301-3>
5. L. Menard, Y. Charon, M. Solal, M. Ricard, P. Laniece, R. Mastrippolito, L. Pinot, L. Valentin, Performance characterization and first clinical evaluation of intra-operative compact gamma imager, *IEEE Trans. Nucl. Sci.*, Vol. 46, No 6, (1999), pp 2068 – 2074 Available: http://ieeexplore.ieee.org/xpl/articleDetails.jsp?arnumber=819284&sortType%3Dasc_p_Sequence%26filter%3DAND%28p_IS_Number%3A17754%29
6. N. Uzunov, M. Bello, P. Boccaccio, G. Moschini, G. Baldazzi, D. Bollini, F. de Notaristefani, U. Mazzi, M. Riondato, Performance measurements of a high-spatial-resolution YAP camera, *Phys. Med. Biol.*, 50 (2005), N11 – N21 Available: <http://iopscience.iop.org/0031-9155/50/3/N01>
7. Position sensitive photomultiplier tubes with crossed wire anodes R2486 ser. Hamamatsu Tech. Data, TPMH1206E01, Jul. 1998, Japan.